Utility of computed diffusion-weighted MRI for predicting aggressiveness of prostate cancer

Waseda, Yuma; Yoshida, Soichiro; Takahara, Taro; Kwee, Thomas Christian; Matsuoka, Yoh; Saito, Kazutaka; Kihara, Kazunori; Fujii, Yasuhisa

Published in:
Journal of Magnetic Resonance Imaging

DOI:
10.1002/jmri.25593

Publication date:
2017

Utility of Computed Diffusion-Weighted MRI for Predicting Aggressiveness of Prostate Cancer

Yuma Waseda, MD,[1] Soichiro Yoshida, MD, PhD,[1]* Taro Takahara, MD, PhD,[2] Thomas Christian Kwee, MD, PhD,[3] Yoh Matsuoka, MD, PhD,[1] Kazutaka Saito, MD, PhD,[1] Kazunori Kihara, MD, PhD,[1] and Yasuhisa Fujii, MD, PhD[1]

Purpose: To investigate the value of computed (c) diffusion-weighted imaging (DWI) in assessing prostate cancer aggressiveness.
Materials and Methods: Fifty-five patients with peripheral zone prostate cancer who underwent prebiopsy 1.5T magnetic resonance imaging (including native DWI at *b*-values of 0 and 1000 s/mm^2) were included. cDWI signal intensities of peripheral zone prostate cancer and nonmalignant prostate tissue were measured. Association between changes in monoexponentially calculated cDWI signals according to different *b*-values and primary Gleason grades were assessed.
Results: The cDWI signal intensity of prostate cancer was lower at $b = 0$ s/mm^2 and higher at $b = 1000$ s/mm^2 compared to nonmalignant prostate tissue. The *b*-value at which the signal intensities of prostate cancer and nonmalignant prostate tissue were equal was defined as the "iso-*b*-value." On multivariate analysis, only the iso-*b*-value was a significant predictor of primary Gleason grade 4/5 cancer ($P = 0.001$). The area under the curve (AUC) of the iso-*b*-value for diagnosing primary Gleason grade 4/5 cancer was 0.94, and significantly higher than that of the tumor apparent diffusion coefficient (ADC) value with an AUC of 0.68 ($P < 0.001$).
Conclusion: cDWI with iso-*b*-value-based semiquantitative analysis was found to be useful for predicting the aggressiveness of prostate cancer and may potentially outperform tumor ADC measurements in this setting.
Level of Evidence: 3
Technical Efficacy: Stage 2

J. MAGN. RESON. IMAGING 2017;46:490–496

Accurate assessment of tumor aggressiveness of localized prostate cancer is critical for optimal treatment selection. Treatment strategies of localized prostate cancer vary widely from active surveillance,[1,2] to focal treatment,[3,4] and radical whole-gland therapy. The Gleason grade reflects prostate cancer aggressiveness and predicts clinical course.[5,6] Gleason grade as determined by biopsy, however, has been reported to undergrade prostate cancer in a substantial proportion of patients,[7,8] which could potentially result in a suboptimal therapeutic strategy.[9]

Diffusion-weighted imaging (DWI) is a functional magnetic resonance imaging (MRI) technique that quantifies the diffusion of water molecules in tissues without using any contrast agents, radiotracers, or exposure to ionizing radiation. DWI has become an essential sequence for detecting prostate cancer. The utility of DWI as an imaging biomarker for characterizing prostate cancer has been shown by several recent studies.[10,11] The apparent diffusion coefficient (ADC) is a quantitative marker that reflects the magnitude of water diffusion in tissues, and a significant correlation between the ADC value and Gleason grade has been reported.[12–14] Nevertheless, ADC measurement has an intrinsic limitation in that the ADC value depends on the MRI system and imaging protocol.[15,16]

To decrease the impact arising from this limitation, we developed a new semiquantitative method to predict the

View this article online at wileyonlinelibrary.com. DOI: 10.1002/jmri.25593

Received Sep 29, 2016, Accepted for publication Nov 29, 2016.

*Address reprint requests to: S.Y., Urology, Tokyo Medical and Dental University Graduate School, 1-5-45 Yushima, Bunkyo-ku, Tokyo 113-8519, Japan. E-mail: s-yoshida.uro@tmd.ac.jp

From the [1]Urology, Tokyo Medical and Dental University Graduate School, Tokyo, Japan; [2]Biomedical Engineering, Tokai University School of Engineering, Kanagawa, Japan; and [3]Department of Radiology, University Medical Center Groningen, Groningen, Netherlands

TABLE 1. Clinicopathological Characteristics of 55 Prostate Cancer Patients Who Underwent Radical Prostatectomy and Whose Index Cancer Was Located in the Peripheral Zone

Variables	Value
Age (years)	67 (53–78)[a]
Initial PSA, ng/mL	8.72 (4.4–19.8)[a]
Primary Gleason grade	
3	20 (36%)
4/5	32 (58%)/3 (5%)
Clinical T stage on digital rectal examination	
1c	32 (58%)
2/3	17 (31%)/6 (11%)

PSA: prostate specific antigen. Data are shown as *n* (%); [a]median (range).

aggressiveness of prostate cancer in a standardized manner using a computed DWI (cDWI) technique. cDWI is a computational technique that allows synthesizing diffusion-weighted images at any chosen *b*-value from an already acquired DWI dataset that contains at least two *b*-values.[17–19] The cDWI technique allows higher *b*-value DWI to be obtained with good signal-to-noise ratio (SNR) and without additional scan time,[17] which could improve detection and localization of prostate cancer compared to native high *b*-value DWI.[20–23] However, the value of cDWI in determining prostate cancer aggressiveness is still unknown.

The purpose of this study was therefore to investigate the value of cDWI in assessing prostate cancer aggressiveness by determining the association between changes in cDWI signals according to *b*-value manipulation and primary Gleason grades.

Materials and Methods

Patient Selection

Our institutional Ethical Committee approved this retrospective study, and waived the requirement for written informed consent. Between January 2010 and August 2015, 115 patients with prostate-specific antigen (PSA) level less than 20 ng/mL underwent prebiopsy multisequence MRI followed by radical prostatectomy without any neoadjuvant treatment. The index cancer in each patient was defined as the tumor with the highest Gleason score (in case of multiple tumors with the same highest Gleason score in one patient, the largest tumor was selected for this purpose). The index cancer was located in the peripheral zone in 62 patients, and in the transition zone in 53 patients. Of these 62 patients with peripheral zone cancer, 55 whose index cancer was retrospectively identified on prebiopsy MRI in reference to the histological map were eligible for this analysis. The median PSA level of these patients was 8.7 (range; 4.4–19.8) ng/mL. The number of patients with primary Gleason grades of 3, 4, and 5, were 20 (36.4%), 32 (58.2%), and 3 (5.4%), respectively. Clinicopathological data are shown in Table 1.

MRI Technique

Multisequence MRI, including DWI, was performed using a 1.5T system (Intera Achieva; Philips, Best, the Netherlands) with a 32-channel sensitivity encoding body coil under free breathing. For T_2-weighted MRI, the following parameters were used: repetition time (TR), 1500 msec; echo time (TE), 151 msec; matrix, 304×304; field of view (FOV), 250×275 mm; slice thickness, 0.8 mm; interslice gap, 0 mm; number of slices, 110; number of excitations, 1; bandwidth, 620 Hz per pixel. Parameters for DWI with a single-shot echo-planar imaging sequence were set as follows: TR, 5000 msec; TE, 80 msec; matrix, 128×99; FOV, 300×255 mm; slice thickness, 4 mm; interslice gap, 0.4 mm; number of excitations, 3; diffusion gradient encoding in three orthogonal directions; and three different *b*-values ($b = 0$, 1000, and 2000 s/mm^2). ADC maps were generated using a workstation. cDWIs with *b*-values ranging from 0–2000 s/mm^2 (at increments of 100 s/mm^2) were generated from acquired DWI datasets with *b*-values of 0 and 1000 s/mm^2 based on a standard monoexponential fit model, using medical image processing software (OsiriX v. 6.5.1; Pixmeo, Geneva, Switzerland) and its open-source plug-in (Computed DWI Plugin for OsiriX; medITools, Tokyo, Japan).

Histopathological Analysis

The histopathological analysis was done by pathologists who were blinded to the MRI results. Slices of radical prostatectomy specimens were obtained with 4-mm-interval step sections, and all cancer foci were outlined on a histological map. The Gleason grading was assigned according to the 2005 International Society of Urological Pathology consensus conference.[6]

Image Analysis

In each patient, each index cancer focus delineated on the pathological map was identified as a focal area of abnormal signal characterized by low signal intensity on T_2-weighted imaging, high signal intensity on DWI, or low ADC value on the ADC map. A region of interest (ROI) was manually traced to maximally cover the index cancer on the transverse T_2-weighted imaging slice that encompassed the maximal diameter of the cancer. Another ROI was set within the nonmalignant peripheral zone tissue as demonstrated on the pathological map of the radical prostatectomy specimen. ROI placements were done by a urologist (Y.W.) who knew the cancer location, but who was blinded to the corresponding Gleason score. The aforementioned ROIs were then automatically superimposed on the ADC map and each cDWI dataset. In cases in which misalignments were visually obvious due to subtle patient motion, the locations of the ROIs were adjusted manually, without modifying their size or shape. The changes of cDWI signal intensity in the ROI with each *b*-value increment of 100 s/mm^2 were calculated (Fig. 1). The mean ADC value in the ROI was also measured.

Statistical Analysis

Differences between groups were tested with the Wilcoxon rank sum test for continuous variables and the chi-square test for categorical variables. Associations of variables with primary Gleason grade were evaluated by logistic regression analyses. Upon

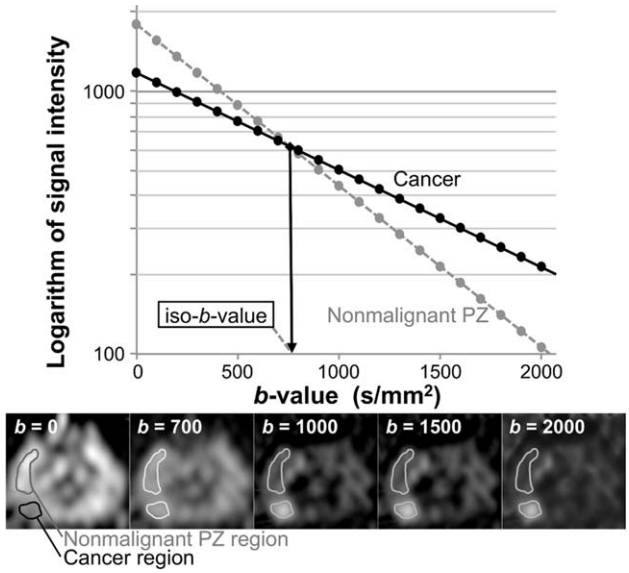

FIGURE 1: Changes of mean signal intensity of cancer and nonmalignant peripheral zone (PZ) according to *b*-value manipulation in a representative case of primary Gleason grade 3 cancer. In all patients, the DWI signal intensities of cancers were lower at $b = 0$ s/mm^2 and higher at $b = 1000$ s/mm^2 than those of nonmalignant peripheral zone tissue regions. We defined the *b*-value at the intersection of the two lines as "iso-*b*-value."

multivariate logistic regression analysis, variables were selected by use of the forward stepwise method. Receiver operating characteristic (ROC) analysis based on logistic regression was performed to assess the diagnostic value of cDWI and ADC measurements for discriminating primary Gleason grade 4/5 from primary Gleason grade 3 cancers. Areas under the ROC curve (AUCs) and optimal cutoff points for maximum accuracy were determined. The sensitivity, specificity, and accuracy of the variables were compared with the McNemar test. All tests were two-sided, with a statistical significance level set at $P < 0.05$. Statistical analyses were performed using the statistical software SPSS v. 20 package (Chicago, IL).

Results

General Imaging Findings

In all patients, the DWI signal intensities of cancer were lower at $b = 0$ s/mm^2 and higher at $b = 1000$ s/mm^2 compared to nonmalignant peripheral zone tissue. The logarithm of mean signal intensities (*y*-axis) against various *b*-values (*x*-axis) decreased linearly for all ROIs. The two lines representing DWI signal of cancer and nonmalignant peripheral zone tissue intersected at one point at which the signal intensities of cancer and nonmalignant peripheral zone tissue were equal. This *b*-value was defined as the "iso-*b*-value." The iso-*b*-value was mathematically calculated from two linear equations according to the following (Fig. 1):

$$\text{iso-}b\text{-value} = 1000 \times [1 + \ln(s_{T1000}/s_{N1000})/\ln(s_{N0}/s_{T0})]^{-1}$$

where s_{N0} and s_{N1000} are signal intensities of nonmalignant prostate tissue on DWI with $b = 0$ and 1000 s/mm^2, respectively; the same applies to s_{T0} and s_{T1000} for prostate cancer.

The iso-*b*-value ranged between 306 and 995 s/mm^2 (median; 637 s/mm^2). The tumor ADC ranged from 0.74×10^{-3} to 1.34×10^{-3} mm^2/s (median; 1.09×10^{-3} mm^2/s) (Table 2).

Pairwise Comparisons of Variables Between Primary Gleason Score 4/5 and 3 Cancers

We compared several clinical and imaging variables between primary Gleason grade 4/5 and 3 cancers (Table 3). There was no significant difference in the area of ROI set in both cancer and nonmalignant peripheral zone between primary Gleason grade 4/5 and primary Gleason grade 3 cancer (33.4 vs. 25.8 mm^2 for cancer, and 133.8 vs. 123.0 mm^2 for nonmalignant peripheral zone). The iso-*b*-value of primary Gleason grade 4/5 cancers was significantly lower than that of primary Gleason grade 3 cancers (550 vs. 737 s/mm^2; $P < 0.001$). The tumor ADC of primary Gleason grade 4/5 cancers was also significantly lower than that of primary Gleason grade 3 cancers (0.62×10^{-3} vs. 0.67×10^{-3} mm^2/s; $P = 0.030$). Accordingly, the iso-*b*-value boxplots showed less overlap in discriminating primary Gleason grade 4/5 from primary Gleason grade 3 cancers than those of tumor ADC (Fig. 2). Of interest, there was also a significant difference in ADCs of nonmalignant peripheral zone tissue between primary Gleason grade 4/5 and primary Gleason grade 3 cancers (1.06×10^{-3} mm^2/s vs. 1.17×10^{-3} mm^2/s; $P = 0.038$). Other comparisons did not show any significant differences between the two groups, although there was a trend ($P = 0.056$) towards a higher initial PSA in primary grade 4/5 cancers.

Univariate, Multivariate, and ROC Analyses for Predicting Primary Gleason Grade 4/5 Cancers

Univariate and multivariate analyses were performed to assess the value of several preoperative characteristics in predicting primary Gleason grade 4/5 cancers (Table 4). Univariate analyses showed that iso-*b*-value ($P = 0.001$) and tumor ADC ($P = 0.036$) were significantly associated with

TABLE 2. Imaging Characteristics of Index Cancer and Nonmalignant Peripheral Zone Tissue

Variables	Value
Area of cancer ROI (mm^2)	28.4 (6.0–123.5)
Tumor ADC ($\times 10^{-3}$ mm^2/s)	0.64 (0.37–0.97)
Area of ROI set in nonmalignant peripheral zone (mm^2)	131.9 (34.4–404.7)
ADC of nonmalignant peripheral zone ($\times 10^{-3}$ mm^2/s)	1.09 (0.74–1.34)
Iso-*b*-value (s/mm^2)	637 (306–995)

ROI: region of interest; ADC: apparent diffusion coefficient. Data are shown as median (range).

TABLE 3. Comparison of Several Clinical and Imaging Variables Between Primary Gleason Grade 3 and 4/5 Cancers

Variables	Primary Gleason grade 3	Primary Gleason grade 4/5	*P* value
No. of patients	20 (36.4%)	35 (63.6%)	
Age (years)	65.5 (62–71.5)	67 (63-71)	0.48
Initial PSA (ng/mL)	8.30 (6.23–9.42)	8.80 (6.29-13.8)	0.056
Area of cancer ROI (mm^2)	25.8 (8.7–104.1)	33.4 (6.0–123.5)	0.68
Tumor ADC ($\times 10^{-3}$ mm^2/s)	0.67 (0.51–0.97)	0.62 (0.37–0.97)	0.030
Area of ROI set in nonmalignant peripheral zone (mm^2)	123.0 (34.4–236.9)	133.8 (36.8–404.7)	0.47
ADC of nonmalignant peripheral zone ($\times 10^{-3}$ mm^2/s)	1.17 (1.04–1.21)	1.06 (1.00–1.15)	0.038
Iso-*b*-value (s/mm^2)	737 (597–995)	550 (306–712)	<0.001

primary Gleason grade 4/5 cancer. On multivariate analysis, only the iso-*b*-value remained as a significant and independent predictor of primary Gleason grade 4/5 cancer ($P = 0.001$; odds ratio 0.97 with 95% confidence interval (CI) of 0.96–0.99 per 1 s/mm^2 increase in *b*-value). The AUC of iso-*b*-value for discriminating primary Gleason grade 4/5 cancer from primary Gleason grade 3 cancer was 0.94 (95% CI: 0.88–1.00), which was significantly higher than that of tumor ADC with an AUC of 0.68 (95% CI: 0.54–0.82) ($P < 0.001$) (Fig. 3). Based on the AUC analysis, the optimal cutoff to discriminate primary Gleason grade 4/5 from 3 cancers was 700 s/mm^2 for iso-*b*-value and 0.83×10^{-3} mm^2/s for tumor ADC. When applying these cutoff values, the sensitivity was good for both (97.1% for iso-*b*-value and 91.2% for tumor ADC, $P = 0.48$), while iso-*b*-value was significantly superior in specificity (70.0%) and accuracy (87.3%) compared to tumor ADC (30.0% and 68.5%, $P = 0.002$ and $P < 0.001$, respectively).

Discussion

The results of this study are the first to show the potential of cDWI-based semiquantitative analysis for preoperative diagnosis of primary Gleason grade 4/5 cancer. The cDWI

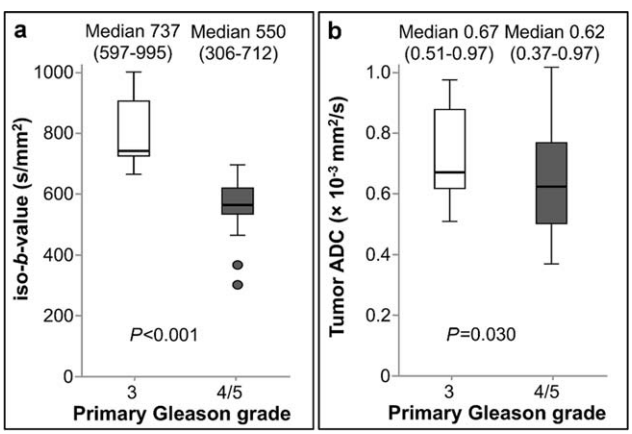

FIGURE 2: Boxplots of iso-*b*-value (a) and ADC value of tumor (b) according to primary Gleason grade (3 vs. 4/5). Center line denotes median, top of box denotes 75th percentile, bottom of box denotes 25th percentile, circles denote outliers (between 1.5 and 3 interquartile ranges). Primary Gleason grade 4/5 cancers had significantly lower iso-*b*-value and tumor ADC than primary Gleason grade 3 cancers (a,b). The iso-*b*-value boxplots showed less overlap in discriminating primary Gleason grade 4/5 from primary Gleason grade 3 cancers than those of tumor ADC.

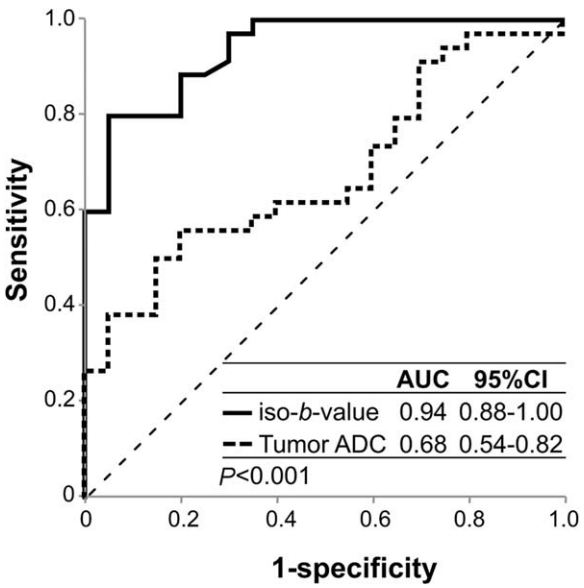

FIGURE 3: ROC analysis for discriminating primary Gleason grade 4/5 cancer from primary Gleason grade 3 cancer for iso-*b*-value and tumor ADC. The AUC of iso-*b*-value was 0.94 (95% CI: 0.88–1.00), which was significantly higher than that of tumor ADC of 0.68 (95% CI: 0.54–0.82) ($P < 0.001$).

TABLE 4. Univariate and Multivariate Analysis of Preoperative Characteristics in Predicting Primary Gleason Score 4/5 Cancers

	Univariate	Multivariate	
		Full model	Reduced model
Variables	***P* value**	***P* value**	***P* value**
Age (years)	0.48	0.30	
PSA (ng/mL)	0.10	0.11	
Abnormal digital rectal examination	0.068	0.96	
Tumor ADC	0.036	0.61	
ADC of nonmalignant peripheral zone	0.074	0.29	
Iso-*b*-value	0.001	0.002	0.001

PSA: prostate-specific antigen; ADC: apparent diffusion coefficient.

technique can generate calculated diffusion-weighted images at any *b*-value, and allows us to observe sequential alterations in DWI signal with changing *b*-value. We showed the associations of both iso-*b*-value and tumor ADC with histological aggressiveness of prostate cancer. Surprisingly, iso-*b*-value was found to be superior to tumor ADC in predicting primary Gleason grade 4/5 cancer, although both parameters were derived from the same DWI dataset that was acquired with only two *b*-values of 0 and 1000 s/mm^2. The explanation for this interesting finding is currently unclear, but may be related to the use vs. nonuse of reference tissue. Tumor ADC is calculated based on the pixels of the tumor only, and it can be affected by shimming quality or local SNR. On the other hand, iso-*b*-value takes into account both the pixels of the tumor and those of the adjacent nonmalignant peripheral zone, both of which should be similarly affected by shimming quality and local SNR. Besides the different physical and mathematical underpinnings between tumor ADC and iso-*b*-value, complex differences in water diffusivity between tumor and adjacent nonmalignant peripheral zone may also play a role. Further investigations are necessary to determine which physical, mathematical, and biological mechanisms have led to the observed different diagnostic values in tumor grading between tumor ADC and iso-*b*-value.

DWI provides functional information based on the degree of water mobility within tissue. DWI is increasingly used for depicting cancerous lesions, on the basis of its high contrast compared with nonmalignant tissue. Higher diffusion weightings can provide higher lesion-to-background contrast, and thus improve tumor detection, as has been shown in various types of tumors including prostate cancer.[24–26] However, higher *b*-value settings under the time constraint in clinical practice could cause severe image distortion and reduce SNR, which results in a marked degradation of image quality with increasing *b*-values. The cDWI technique can generate extrapolated high-*b*-value diffusion-weighted images without additional scan time, based on a DWI dataset that contains at least two different *b*-values. The generated cDWIs provide improved contrast and better SNR compared to acquired DWI datasets, and could improve the detection of prostate cancer, as shown by several recent studies.[20–23] Yet cDWI has not been applied to evaluate prostate cancer aggressiveness.

Although significant correlations between Gleason score and ADC measurements have been reported by several studies, the clinical application of ADC measurements still remains difficult because of a large overlap in ADC values between different Gleason scores.[13,14,27,28] This large overlap may result from a significant variability in ADC values depending on DWI acquisition circumstances (vendor, coil systems, imager, acquisition protocols, and noise)[15,16] and individual patient differences (age, glandular atrophy, cellular density, fibrosis, and alterations in the water content of prostate tissue).[29–31] Some trials have been performed to mitigate this limitation. The utility of standardization of ADC measurements by taking the ratio between the ADC values of cancer and normal reference tissue was reported. Some studies have shown a favorable impact,[32–34] but others did not find any incremental value in using the ADC ratio.[35–37]

The iso-*b*-value is essentially calculated from the signal differences between prostate cancer and normal peripheral zone tissue at low *b*-value DWI and the signal attenuation differences between these two tissues at higher *b*-value DWI. Accordingly, "iso-*b*-value" incorporates the information of DWI signals and ADC values of both cancer and surrounding normal tissue. Incorporating these factors may neutralize the interpatient variation in ADC measurements. Furthermore, background variation of normal peripheral

zone tissue composition has been reported to have a significant impact on the tumor ADC value, as reported by Litjens et al.[32] Of interest, in the present study a nearly significant relationship between the nonmalignant peripheral zone ADC and primary Gleason grade was observed. In this regard, iso-*b*-value has the potential to surpass the utility of tumor ADC value in predicting the aggressiveness of prostate cancer.

For optimal visualization of prostate cancer, a *b*-value higher than 1000 s/mm^2 is recommended to adequately suppress benign prostate tissue background signals.[24] For tumor characterization of prostate cancer, it has also been proposed to select an appropriate *b*-value.[25,26,38] However, no consensus or recommendation exists with regard to the best *b*-value for visually assessing prostate cancer aggressiveness at DWI. The current analysis proposed the optimal *b*-value from the sequential alteration of cDWI signal contrast between prostate cancer and nonmalignant prostate tissue. The iso-*b*-values provided good separation between primary Gleason grade 4/5 cancer and primary Gleason grade 3 cancer, with only small overlap between both groups. The optimal cutoff iso-*b*-value was found to be 700 s/mm^2 in this study. In the current cohort, 97.1% of primary Gleason grade 4/5 cancers showed higher signal intensities than the surrounding nonmalignant tissue, while 70.0% of the primary Gleason grade 3 cancers showed lower signal intensities when employing this iso-*b*-value of 700 s/mm^2. Comparing the signal of prostate cancer with nonmalignant prostate tissue on actually acquired DWI at $b = 700$ s/mm^2 might be a clinically useful simple method to detect aggressive prostate cancer.

We proposed a novel imaging biomarker for characterizing peripheral zone prostate cancer. In the current study, the application of this technique to transition zone cancer was not investigated, which can be regarded as a limitation of the study. However, evaluation of DWI signal in the transition zone is problematic because of stromal nodules of benign prostate hyperplasia. Moreover, the use of $b = 0$ s/mm^2 (along with a high *b*-value of 1000 s/mm^2) for generating ADC maps and cDWI datasets was a possible study limitation. The appropriate conditions for generating ADC maps and cDWI datasets to determine prostate cancer aggressiveness remain unclear. Nevertheless, considering the least amount of time required to acquire DWI with $b = 0$ s/mm^2 compared to other *b*-values, generating cDWIs from *b*-values including $b = 0$ s/mm^2 would be a feasible option for clinical application. Furthermore, we used a single combination of repetition and echo time. Because of maximum gradient strength and slew rate limitations of the current system, and clinical scan time constraints, there was little to no opportunity to vary these parameters. In the future, we may be able to compute not only the *b*-value but also the echo time by acquiring at least two echo times, which could potentially enhance the utility of this method. Other study limitations are the relatively small sample size, the single-center and retrospective design, and possible selection bias. A prospective study in a larger cohort is needed to confirm the current findings.

In conclusion, cDWI with iso-*b*-value-based semiquantitative analysis was found to be useful for predicting the aggressiveness of prostate cancer and may potentially outperform tumor ADC measurements in this setting. Further prospective studies are required to confirm these findings.

References

1. Bill-Axelson A, Holmberg L, Ruutu M, et al. Radical prostatectomy versus watchful waiting in early prostate cancer. N Engl J Med 2005;352:1977–1984.
2. Klotz L, Vesprini D, Sethukavalan P, et al. Long-term follow-up of a large active surveillance cohort of patients with prostate cancer. J Clin Oncol 2015;33:272–277.
3. Ahmed HU, Hindley RG, Dickinson L, et al. Focal therapy for localised unifocal and multifocal prostate cancer: A prospective development study. Lancet Oncol 2012;13:622–632.
4. Smith DW, Stoimenova D, Eid K, Barqawi A. The role of targeted focal therapy in the management of low-risk prostate cancer: update on current challenges. Prostate Cancer 2012;2012:587139.
5. Gleason DF, Mellinger GT, Prediction of prognosis for prostatic adenocarcinoma by combined histological grading and clinical staging. J Urol 1974;111:58–64.
6. Epstein JI, Allsbrook WCJ, Amin MB, Egevad LL. The 2005 International Society of Urological Pathology (ISUP) Consensus Conference on Gleason Grading of Prostatic Carcinoma. Am J Surg Pathol 2005;29:1228–1242.
7. Legmann P, Zerbib M, Delongchamps NB. Gleason score determination with transrectal ultrasound-magnetic resonance imaging fusion guided prostate biopsies. Are we gaining in accuracy? 2016;195:88–93.
8. Epstein JI, Feng Z, Trock BJ, Pierorazio PM. Upgrading and downgrading of prostate cancer from biopsy to radical prostatectomy: incidence and predictive factors using the modified Gleason grading system and factoring in tertiary grades. Eur Urol 2012;61:1019–1024.
9. Etzioni R, Penson DF, Legler JM, et al. Overdiagnosis due to prostate-specific antigen screening: lessons from U.S. prostate cancer incidence trends. J Natl Cancer Inst 2002;94:981–990.
10. Tanimoto A, Nakashima J, Kohno H, Shinmoto H, Kuribayashi S. Prostate cancer screening: the clinical value of diffusion-weighted imaging and dynamic MR imaging in combination with T2-weighted imaging. J Magn Reson 2007;25:146–152.
11. Selnæs KM, Heerschap A, Jensen LR, et al. Peripheral zone prostate cancer localization by multiparametric magnetic resonance at 3T: unbiased cancer identification by matching to histopathology. Invest Radiol 2012;47:624–633.
12. Tamada T, Sone T, Jo Y, et al. Apparent diffusion coefficient values in peripheral and transition zones of the prostate: comparison between normal and malignant prostatic tissues and correlation with histologic grade. J Magn Reson Imaging 2008;28:720–726.
13. deSouza NM, Riches SF, VanAs NJ, et al. Diffusion-weighted magnetic resonance imaging: a potential non-invasive marker of tumour aggressiveness in localized prostate cancer. Clin Radiol 2008;63:774–782.
14. Vargas HA, Akin O, Franiel T, et al. Diffusion-weighted endorectal MR imaging at 3T for prostate cancer: tumor detection and assessment of aggressiveness. Radiology 2011;259:775–784.
15. Sasaki M, Yamada K, Watanabe Y, et al. Variability in absolute apparent diffusion coefficient values across different platforms may be

substantial: a multivendor, multi-institutional comparison study. Radiology 2008;249:624–630.

16. Döpfert J, Lemke A, Weidner A, Schad LR. Investigation of prostate cancer using diffusion-weighted intravoxel incoherent motion imaging. Magn Reson Imaging 2011;29:1053–1058.
17. Blackledge MD, Leach MO, Collins DJ, Koh D-M. Computed diffusion-weighted MR imaging may improve tumor detection. Radiology 2011;261:573–581.
18. Maas MC, Fütterer JJ, Scheenen TWJ. Quantitative evaluation of computed high B value diffusion-weighted magnetic resonance imaging of the prostate. Invest Radiol 2013;48:779–786.
19. Ueno Y, Takahashi S, Ohno Y, et al. Computed diffusion-weighted MRI for prostate cancer detection: The influence of the combinations of b-values. Br J Radiol 2015;88.
20. Ueno Y, Takahashi S, Kitajima K, et al. Computed diffusion-weighted imaging using 3-T magnetic resonance imaging for prostate cancer diagnosis. Eur Radiol 2013;23:3509–3516.
21. Vural M, Ertas G, Onay A, et al. Conspicuity of peripheral zone prostate cancer on computed diffusion-weighted imaging: Comparison of cDWI1500, cDWI2000, and cDWI3000. Biomed Res Int 2014;2014.
22. Bittencourt LK, Attenberger UI, Lima D, et al. Feasibility study of computed vs measured high b-value (1400 s/mm^2) diffusion-weighted MR images of the prostate. World J Radiol 2014;6:374–380.
23. Rosenkrantz AB, Chandarana H, Hindman N, et al. Computed diffusion-weighted imaging of the prostate at 3T: Impact on image quality and tumour detection. Eur Radiol 2013;23:3170–3177.
24. Padhani AR, Liu G, Koh DM, et al. Diffusion-weighted magnetic resonance imaging as a cancer biomarker: consensus and recommendations. Neoplasia 2009;11:102–125.
25. Katahira K, Takahara T, Kwee TC, et al. Ultra-high-b-value diffusion-weighted MR imaging for the detection of prostate cancer: Evaluation in 201 cases with histopathological correlation. Eur Radiol 2011;21:188–196.
26. Metens T, Miranda D, Absil J, Matos C. What is the optimal b value in diffusion-weighted MR imaging to depict prostate cancer at 3T? Eur Radiol 2012;22:703–709.
27. Verma S, Rajesh A, Morales H, et al. Assessment of aggressiveness of prostate cancer: Correlation of apparent diffusion coefficient with histologic grade after radical prostatectomy. Am J Roentgenol 2011;196:374–381.
28. Itou Y, Nakanishi K, Narumi Y, Nishizawa Y, Tsukuma H. Clinical utility of apparent diffusion coefficient (ADC) values in patients with prostate cancer: Can ADC values contribute to assess the aggressiveness of prostate cancer? J Magn Reson Imaging 2011;33:167–172.
29. Tamada T, Sone T, Toshimitsu S, et al. Age-related and zonal anatomical changes of apparent diffusion coefficient values in normal human prostatic tissues. J Magn Reson Imaging 2008;27:552–556.
30. Ren J, Huan Y, Wang H, et al. Diffusion-weighted imaging in normal prostate and differential diagnosis of prostate diseases. Abdom Imaging 2008;33:724–728.
31. Gibbs P, Liney GP, Pickles MD, Zelhof B, Rodrigues G, Turnbull LW. Correlation of ADC and T2 measurements with cell density in prostate cancer at 3.0 Tesla. Invest Radiol 2009;44:572–576.
32. Litjens GJS, Hambrock T, Hulsbergen-van de Kaa C, Barentsz JO, Huisman HJ. Interpatient variation in normal peripheral zone apparent diffusion coefficient: effect on the prediction of prostate cancer aggressiveness. Radiology 2012;265:260–266.
33. Lebovici A, Sfrangeu SA, Feier D, et al. Evaluation of the normal-to-diseased apparent diffusion coefficient ratio as an indicator of prostate cancer aggressiveness. BMC Med Imaging 2014;14:15.
34. Boesen L, Chabanova E, Løgager V, Balslev I, Thomsen HS. Apparent diffusion coefficient ratio correlates significantly with prostate cancer gleason score at final pathology. J Magn Reson Imaging 2015;42:446–453.
35. De Cobelli F, Ravelli S, Esposito A, et al. Apparent diffusion coefficient value and ratio as noninvasive potential biomarkers to predict prostate cancer grading: Comparison with prostate biopsy and radical prostatectomy specimen. Am J Roentgenol 2015;204:550–557.
36. Rosenkrantz AB, Khalef V, Xu W, Babb JS, Taneja SS, Doshi AM. Does normalisation improve the diagnostic performance of apparent diffusion coefficient values for prostate cancer assessment?. A blinded independent-observer evaluation. Clin Radiol 2015;70:1032–1037.
37. Woo S, Kim SY, Cho JY, Kim SH. Preoperative evaluation of prostate cancer aggressiveness: using ADC and ADC ratio in determining Gleason score. AJR Am J Roentgenol 2016;207:114–120.
38. Peng Y, Jiang Y, Antic T, et al. Apparent diffusion coefficient for prostate cancer imaging: Impact of b values. Am J Roentgenol 2014;202.